Supplementary Figures

1

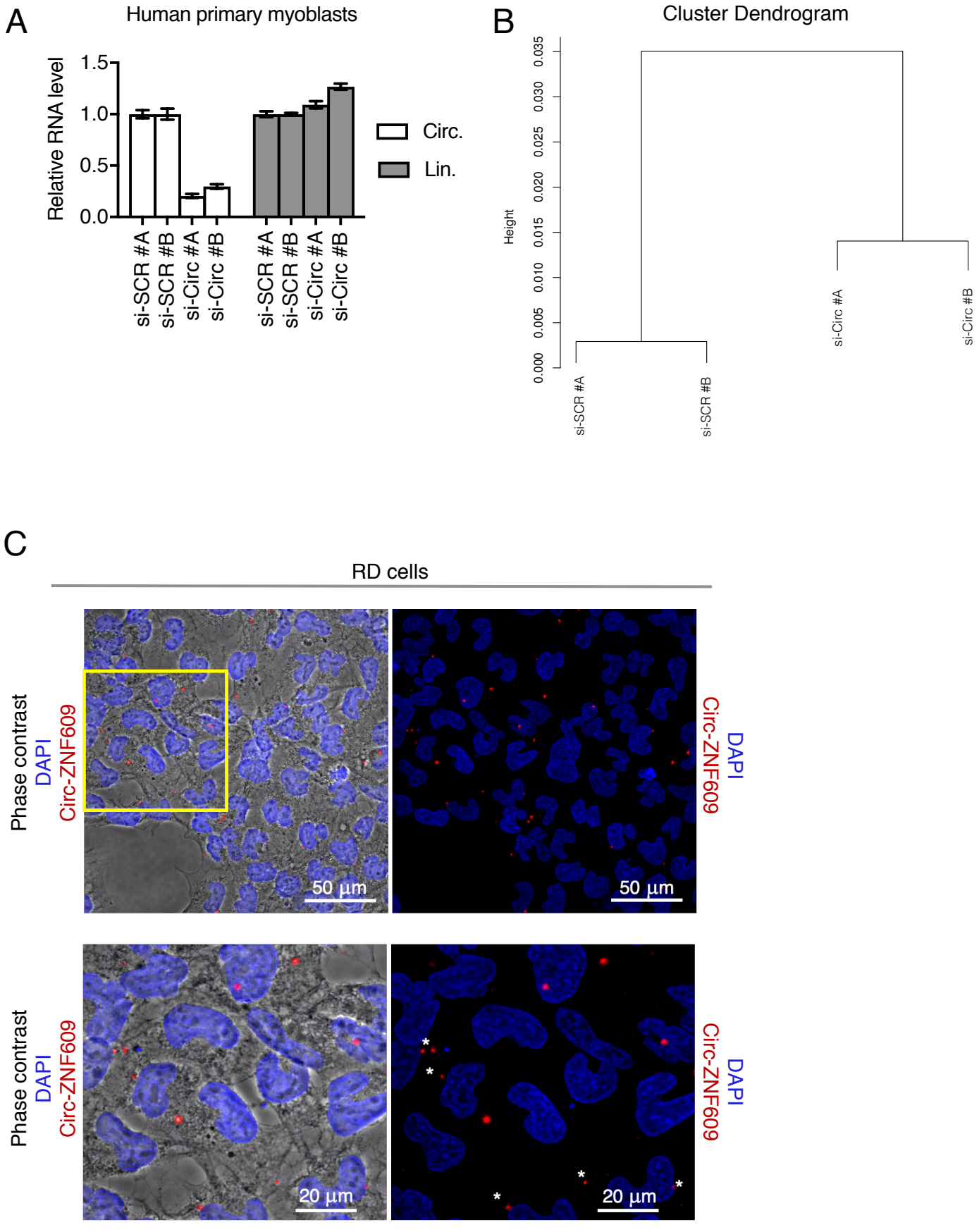

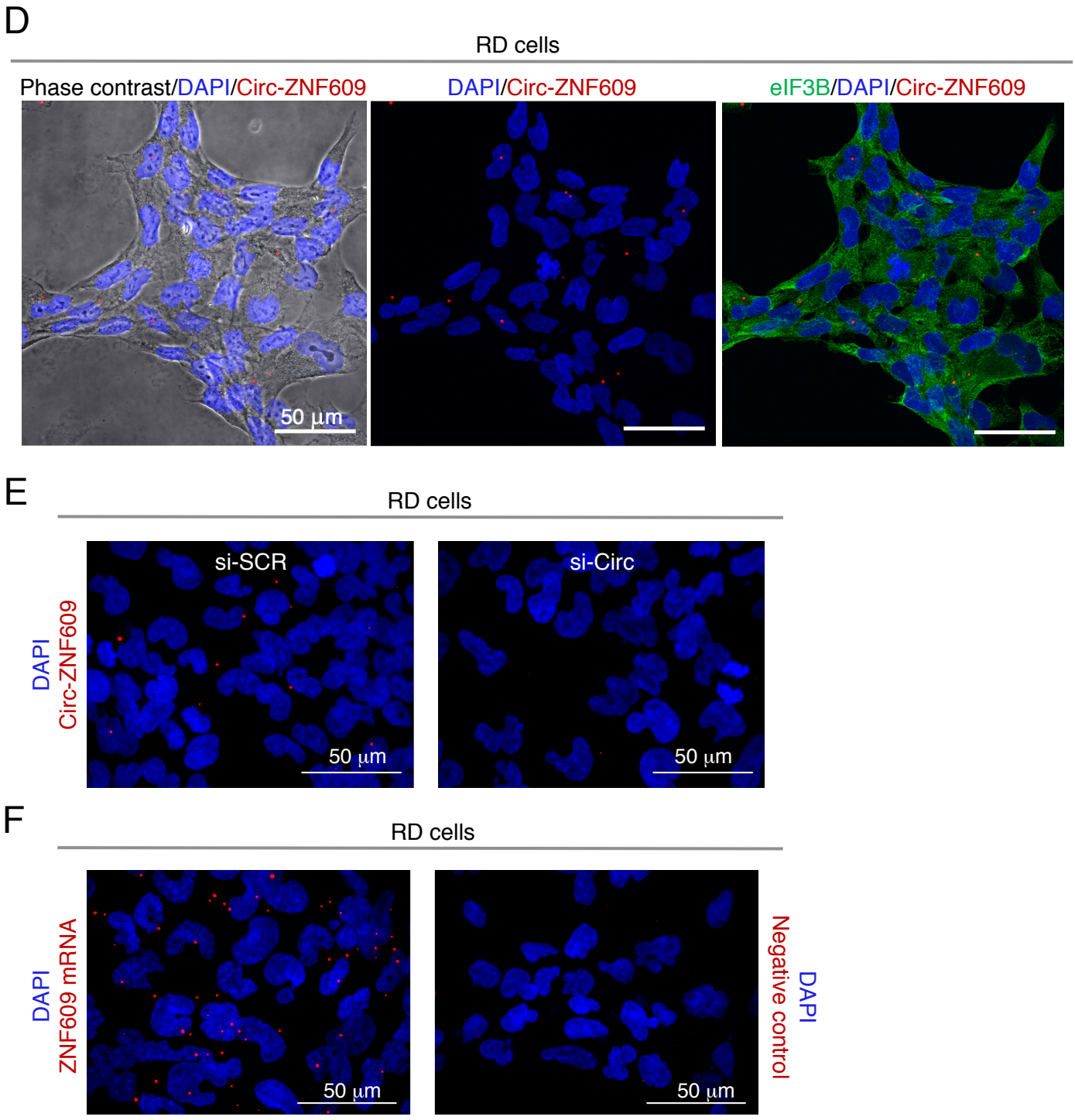

Figure S1

A. RNA levels measured by qRT-PCR of circ-ZNF609 (Circ.) and ZNF609 (Lin.) in human primary myoblasts treated either with control siRNA (si-SCR) or with si-Circ and sent for the RNA-seq analysis. Data are shown as means ± standard error of technical duplicates. N=2.
B. Hierarchical clustering of samples based on Pearson correlation of gene expression profiles in human primary myoblasts treated either with si-SCR (si-SCR #A and #B) or with si-Circ (si-Circ #A and #B).
C. FISH in RD cells using a circ-ZNF609-specific probe (red staining): on the left, merged image with DAPI staining, circ-ZNF609 staining and phase contrast to highlight cell borders; on the right, merged image with only DAPI staining and circ-ZNF609 staining. In the yellow square there is the image area zoomed in the lower panel. White asterisks indicate smaller circ-ZNF609 spots.
D. FISH using a circ-ZNF609-specific probe (red staining) combined to eIF3B immunofluorescence (green staining), in RD cells; left panel: merged image with DAPI staining, circ-ZNF609 staining and phase contrast; central panel: merged image with DAPI staining and circ-ZNF609 staining; right panel: merged image with DAPI staining, circ-ZNF609 staining and eIF3B staining.
E. FISH in RD cells using a circ-ZNF609-specific probe (red staining), in si-SCR and si-Circ.
F. FISH in RD cells using either a ZNF609-specific probe (left) or a bacterial-specific probe ("negative control", right).

Supplementary Figures

2

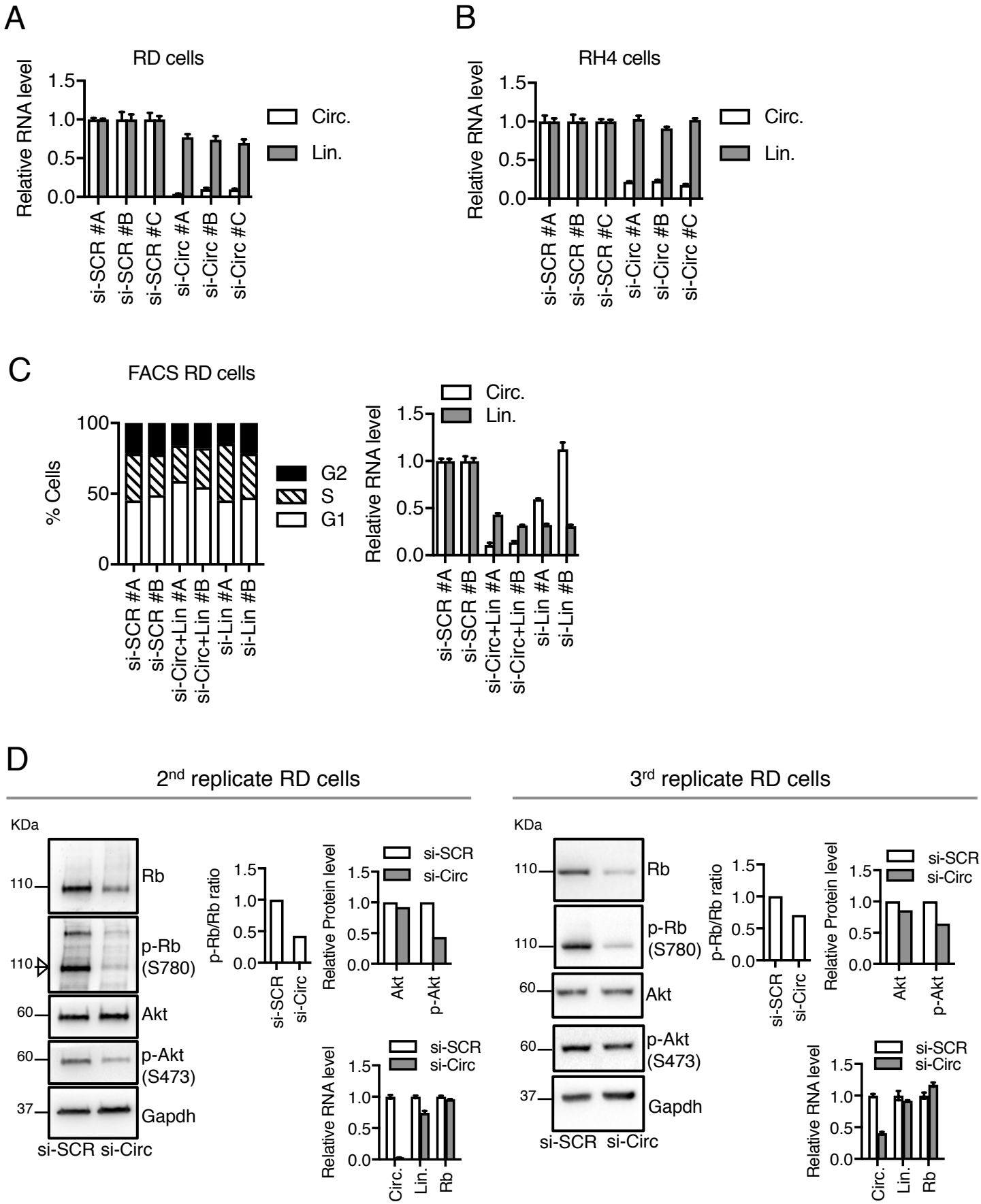

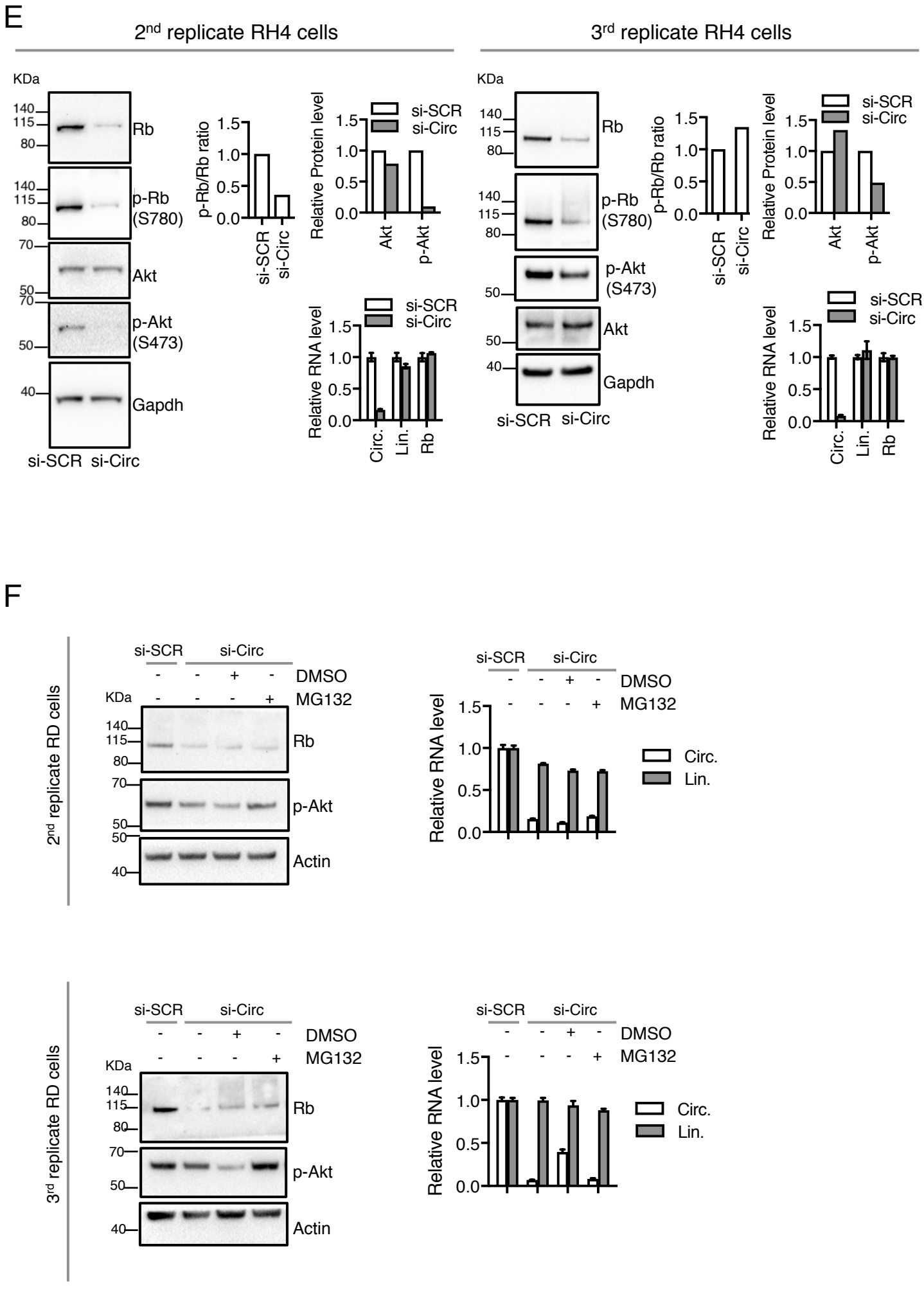
E
2nd replicate RH4 cells
3rd replicate RH4 cells
KDa
Rb
p-Rb (S780)
Akt
p-Akt (S473)
Gapdh
si-SCR
si-Circ
p-Rb/Rb ratio
Relative Protein level
Relative RNA level
Akt
p-Akt
Circ.
Lin.
Rb
F
2nd replicate RD cells
3rd replicate RD cells
DMSO
MG132
p-Akt
Actin
Circ.
Lin.

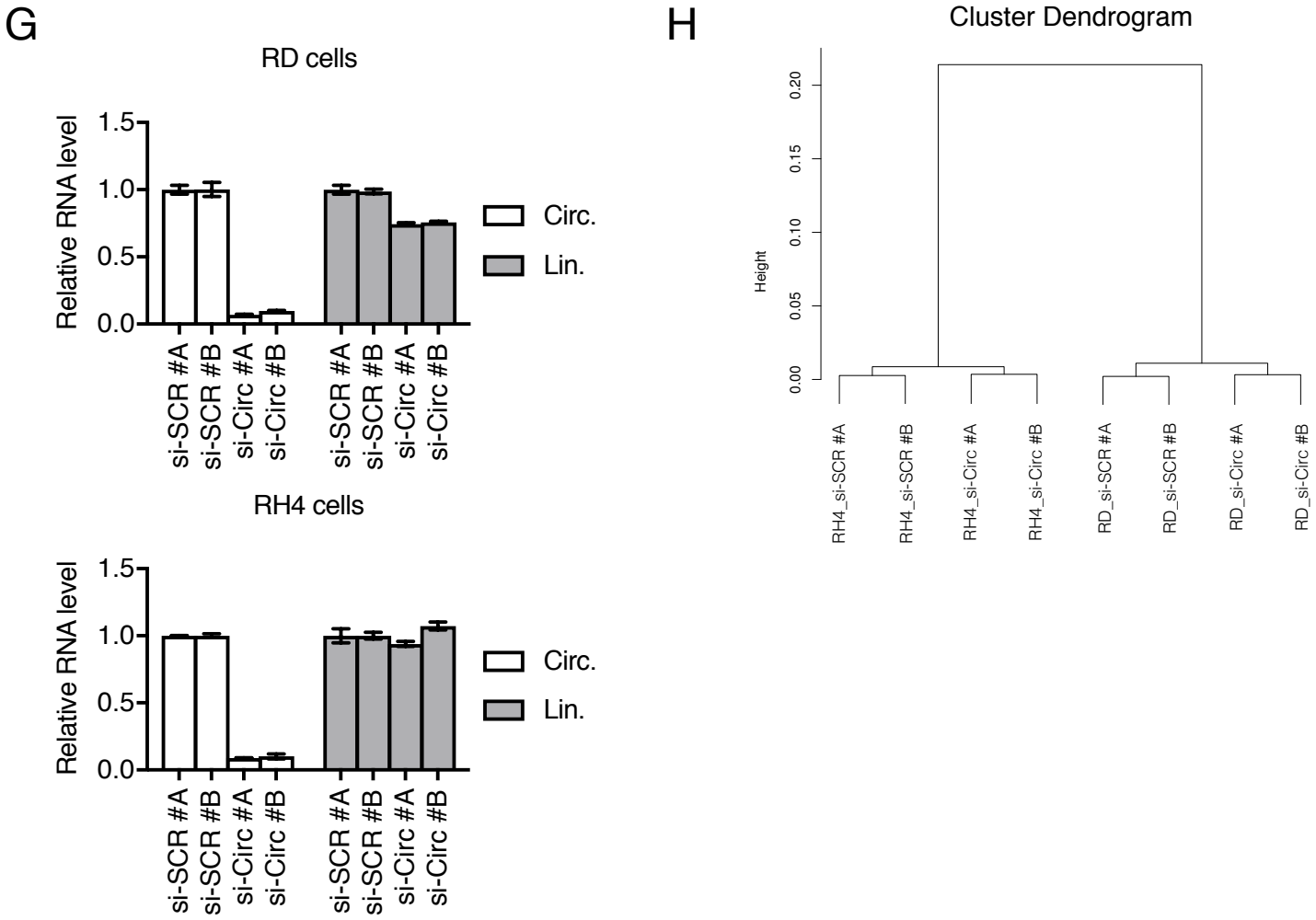

Figure S2

A. RNA levels measured by qRT-PCR of circ-ZNF609 (Circ.) and ZNF609 (Lin.) in three replicates (#A, #B and #C) of RD cells treated with either si-SCR or si-Circ and analyzed for FACS cell cycle analysis. Data are shown as means ± standard error of technical duplicates. N=3.
B. RNA levels measured by qRT-PCR of circ-ZNF609 (Circ.) and ZNF609 (Lin.) in three replicates (#A, #B and #C) of RH4 cells treated with either si-SCR or si-Circ and analyzed for FACS cell cycle analysis. Data are shown as means ± standard error of technical duplicates. N=3.
C. Left: cell cycle analysis by flow cytometry (FACS) of RD cells treated with either si-SCR or si-Circ+Lin or si-Lin. N=2. Right: corresponding RNA levels measured by qRT-PCR of circ-ZNF609 (Circ.) and ZNF609 (Lin.). qRT-PCR data are shown as means ± standard error of technical duplicates. The experiment was repeated at least twice.
D. - E. Two additional independent western blots in RD (**D**) and RH4 (**E**) cells, in si-SCR and si-Circ conditions (Gapdh hybridization was used as loading control). Corresponding ratio of pRb/Rb protein levels, Akt and p-Akt protein levels (relative to Gapdh) and RNA levels (measured by qRT-PCR of circ-ZNF609 (Circ.), ZNF609 (Lin.) and Rb) are shown. qRT-PCR data are shown as means ± standard error of technical duplicates. The experiment was repeated at least three times (N=3).
F. Two additional independent replicates of proteasome inhibition experiment in RD cells treated with either si-SCR or si-Circ: western blot and RNA analysis by qRT-PCR of circ-ZNF609 (Circ.) and ZNF609 (Lin.). qRT-PCR data are shown as means ± standard error of technical duplicates.
G. RNA levels measured by qRT-PCR of circZNF609 (Circ.) and ZNF609 (Lin.) in two replicates (#A and #B) of RD and RH4 cells treated with either si-SCR or si-Circ and sent for RNA-Seq analysis. Data are shown as means ± standard error of technical duplicates.
H. Hierarchical clustering of samples based on Pearson correlation of gene expression profiles in RD and RH4 cells treated either with si-SCR (si-SCR #A and #B) or with si-Circ (si-Circ #A and #B).

Supplementary Figures

3

A

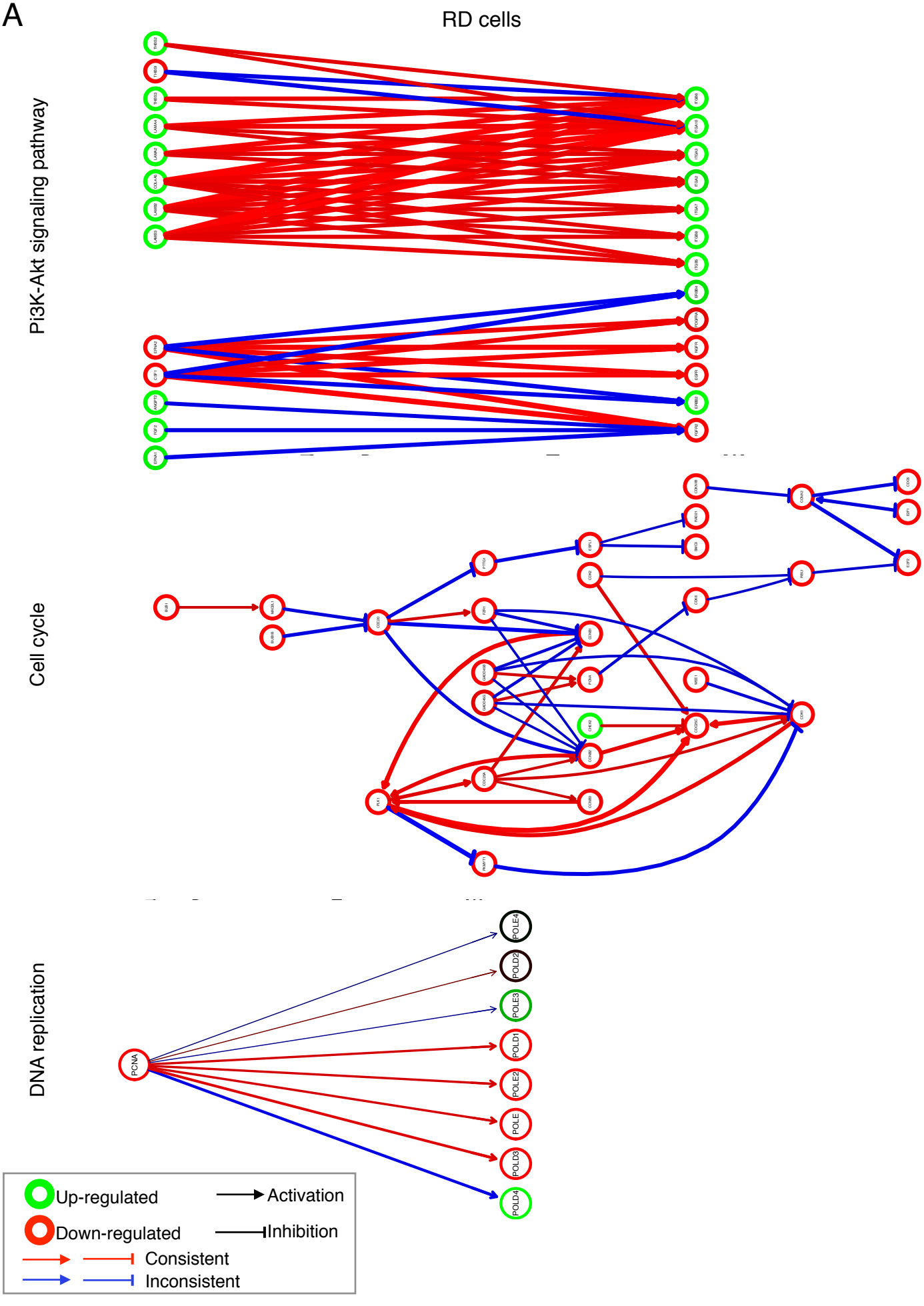

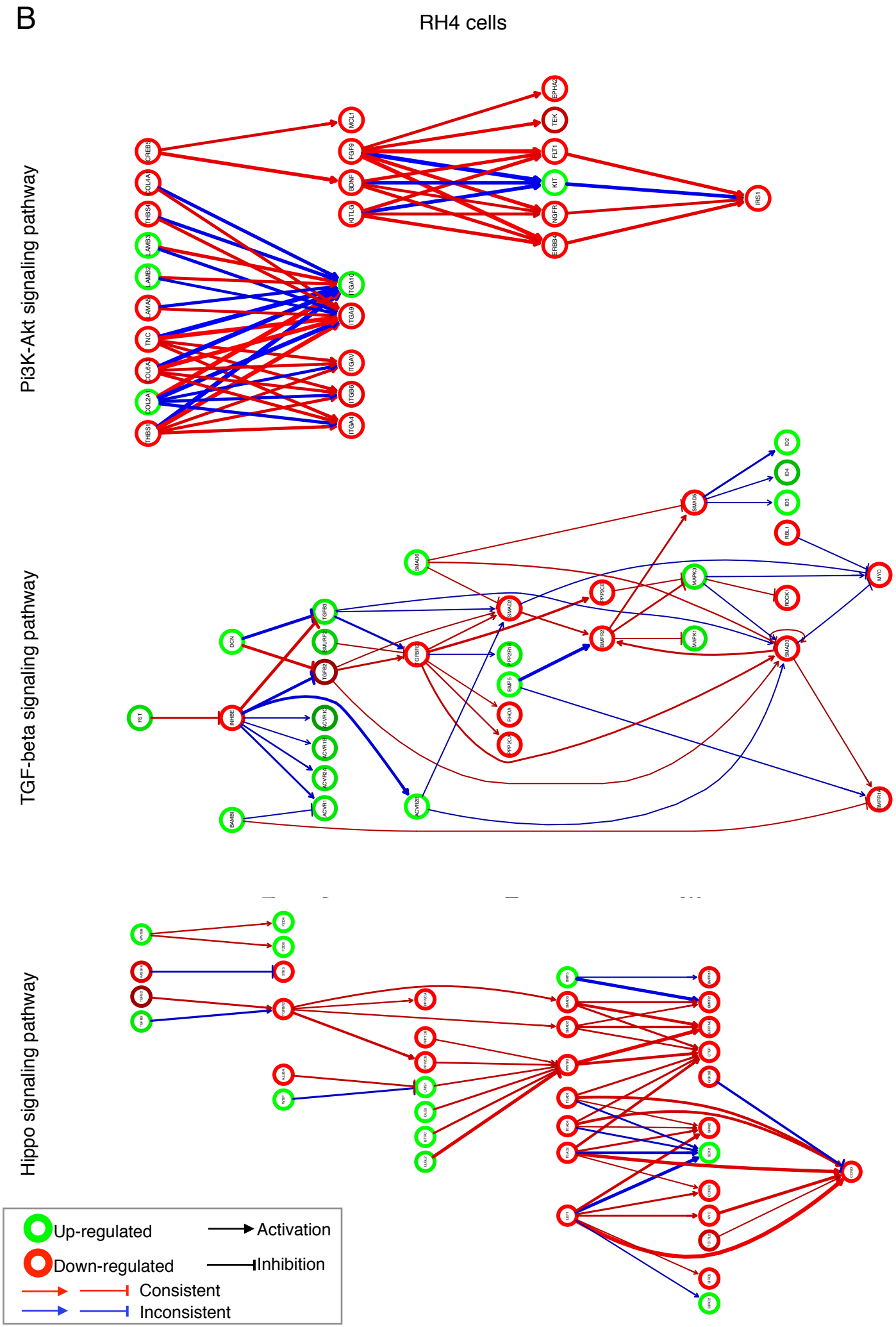
B
RH4 cells
Pi3K-Akt signaling pathway
TGF-beta signaling pathway
Hippo signaling pathway
Up-regulated
Down-regulated
Activation
Inhibition
Consistent
Inconsistent

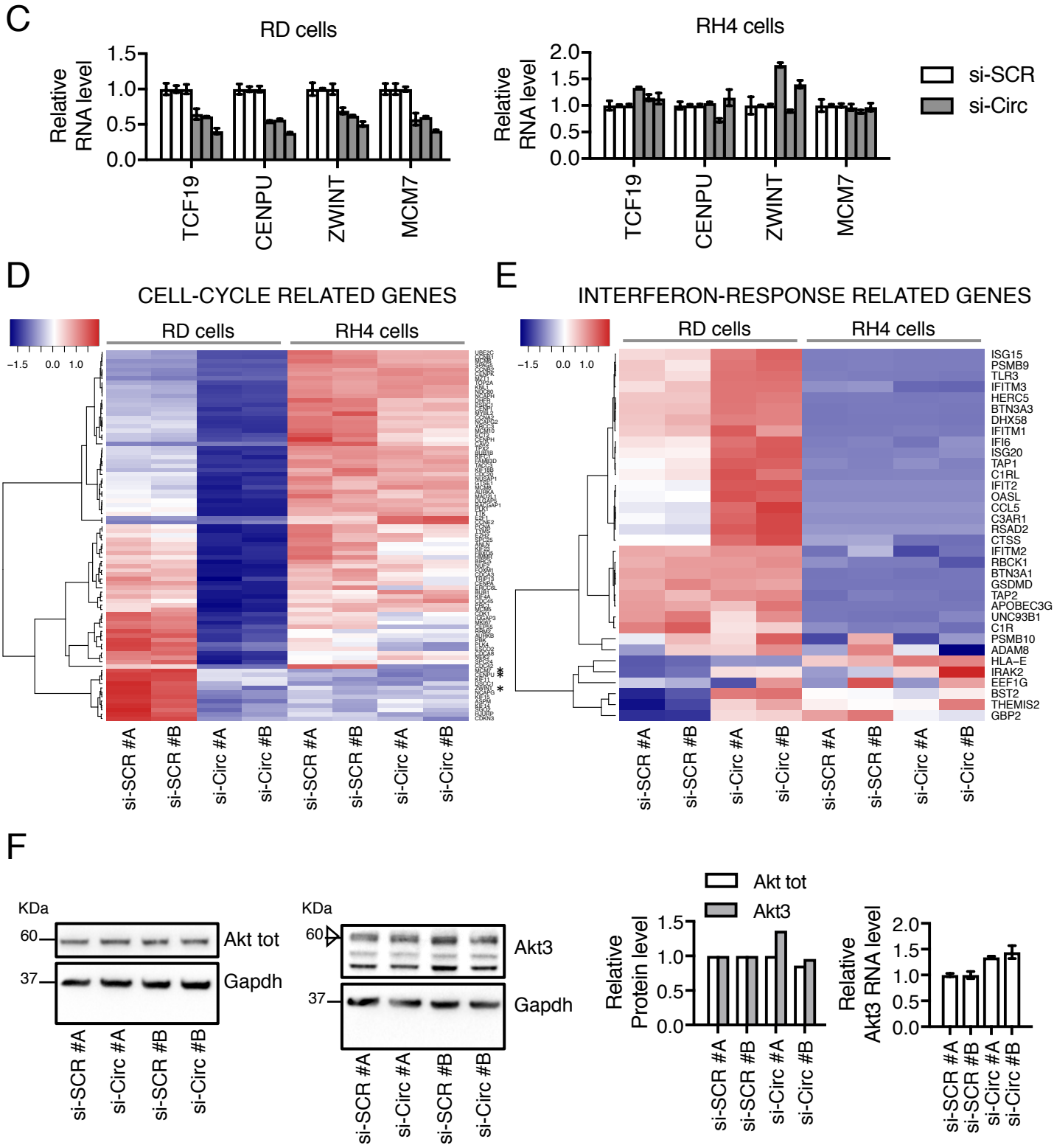

Figure S3

A. Some of the most significant GGEA (Gene Graph Enrichment Analysis) results for RD cells (si-SCR vs si-Circ). The clearer the node/edge colour appears, the more significant it is.
B. Some of the most significant GGEA (Gene Graph Enrichment Analysis) results for RH4 cells (si-SCR vs si-Circ). The clearer the node/edge colour appears, the more significant it is.
C. RNA levels measured by qRT-PCR of some master regulators identified though msVIPER analysis, in RD and RH4 cells, in si-SCR and si-Circ. Data are shown as means ± standard error of technical duplicates. N=3.
D. - E. Heatmaps representing differential expression of some cell-cycle related genes (**D**) and some interferon-response related genes (**E**) in RD and RH4 cells in si-SCR and si-Circ, in two replicates (#A and #B) analyzed by RNA-Seq. Expression values are plotted as colour-coded mean-centered log2-transformed RPKM values.
F. Western blot analysis of total Akt and Akt3 levels in two independent replicates (#A and #B) of RD cells treated with either si-SCR or si-Circ; corresponding protein levels (relative to Gapdh) and RNA analysis. qRT-PCR data are shown as means ± standard error of technical duplicates. N=2.

Legend of Supplementary Tables

S1_Differentially expressed genes
Results of differential expression analyses performed using edgeR software in human primary myoblasts (si-SCR/si-Circ), in RD cells (si-SCR/si-Circ), in RH4 cells (si-SCR/si-Circ) and in RD/RH4 cells.

S2_Interferon gene expression
RNA levels of some isoforms of Interferon Alpha (IFN-A) and Beta (IFN-B) expressed in human primary myoblasts were measured by qRT-PCR in a time-course of 6-12-24-48h after either si-SCR or si-Circ transfection. HPRT mRNA was used as a reference target. The table contains Ct (threshold cycle) means of technical replicates. N=2.

S3_GGEA_rank
Gene Graph Enrichment Analysis (GGEA) results for RD cells (in si-SCR and si-Circ conditions) and RH4 cells (in si-SCR and si-Circ conditions).

S4_Oligonucleotides
List of oligonucleotide pairs (FW and RV) used in this work.

S5_Read_Number
Number of reads and mapping statistics for myoblast and RMS samples analyzed by RNA-Seq in this work.

Supplementary materials and methods

RNA-Seq, bioinformatics analysis and statistics

Total RNA was extracted as described before and treated with DNase I (New England Biolabs, Ipswich, MA, USA) according to the manufacturer's protocol. 2 biological replicates for each condition were performed for RNA-Seq in human primary myoblasts and in RMS samples. Total RNA was sequenced on an Illumina Hiseq 2500 Sequencing system using TruSeq Stranded Total RNA Library Prep Kit with Ribo-Zero treatment at the Institute of Applied Genomics (IGA; Udine, Italy). An average of about 13 million and 30 million 125-nucleotide long paired-end reads were produced for myoblast and RMS samples, respectively. Adapter sequences and poor quality ends were removed using the Trimmomatic software (53); reads with length < 20 nt after trimming were filtered out. Reads were mapped to human GRCh38 genome and Ensembl 90 transcriptome (54) using STAR software (55), with parameters *--outSAMstrandField intronMotif --outFilterType BySJout --outFilterMultimapNmax 20 --alignSJoverhangMin 8 --alignSJDBoverhangMin 1 --outFilterMismatchNmax 999 --outFilterMismatchNoverLmax 0.04 --outFilterIntronMotifs RemoveNoncanonic*al. Number of reads and mapping statistics are reported in Table S5. Htseq-count software (56) was used to count reads mapping to Ensembl 90 human genes; the overlap resolution mode was set to *intersection-strict*. Differential gene expression was performed using edgeR R package (57) after filtering out genes with a CPM (Count Per Million) value less than 1 in at least two samples. edgeR software is particularly suited for experiments with few replicates (58). TMM normalization was applied independently for myoblast and RMS samples. Pearson correlation-based sample hierarchical clusterings, as well as gene expression heatmaps were drawn based on log2-transformed RPKM values, calculated using the edgeR *rpkm* function. Model fitting and testing were performed using *glmFIT* and *glmLRT* functions. FDR cutoff for selecting significant differentially expressed genes was set to 0.05 and absolute log2 fold change was set to > 0.5. Gene Ontology (GO) terms (59) and Reactome pathways (45) enrichment analyses were performed using WebGestalt web server (60) and all genes tested for differential expression as a background; an adjusted p-value cutoff of 0.05 was used to select enriched categories. EnrichmentBrowser R package (61) was employed to perform KEGG pathways (32) based Gene Graph Enrichment analysis (31), using an absolute log2 fold change significance level equal to 0.5 and a statistical significance level equal to 0.05. Transcriptional regulator activity analysis was performed through msviper function included in the Viper R package (33) using RPKMs as expression values; the ARACNe-AP-inferred (62) human sarcoma (63) regulon used in the analysis was taken from the aracne.networks R package, available at https://bioconductor.org/packages/release/data/experiment/html/aracne.networks.html. A p-value cutoff of 0.05 was used to filter results, which were then ranked based on p-value; the top 30 transcriptional regulators were used to draw the msVIPER analysis plot.

Fluorescent in situ hybridization

The cells were cultured on pre-coated glass coverslips (0,4 mg/ml Collagen Rat Tail, Corning) and then fixed in 4% paraformaldehyde/PBS (Electron Microscopy Sciences, Hatfield, PA) for 20 min at 4°C. After dehydration steps with ice-cold Ethanol series (50%, 70%, 100%), cells were stored at -20°C in absolute ethanol until use. Detection of circular ZNF609 RNA was performed using Basescope assay (Advanced Cell Diagnostics, Bio-Techne) in accordance with the manufacturer's instructions, with a little modification. Briefly, fixed cells were permeabilized with Protease III (diluted 1:15) before hybridization with BA-HS-ZNF609circRNA-1ZZ-Exon1 probe (ref. 708461), designed by ACD and ordered as a single-plex probe to detect back-splice junction of the circular molecule. A probe specific for exon junction Exon2-Exon3 of ZNF609 mRNA (BA-HS-ZNF609linearRNA-1ZZ- Exon2-3 probe, ref. 798471) and for bacterial RNA dapB, were used as positive and negative controls, respectively. The cells were incubated with probe solution (45ul for each coverslip) at 40°C for 2 hour in the EZ Hybridization oven using the humidity control tray and slide rack (ACD Instruments). Amplification and detection steps were performed using Basescope detection reagents – RED (ref. 322910) and SIGMAFAST™ Fast Red TR/Naphthol AS-MX Tablets (Sigma-Aldrich) for fluorescent signal development. The washings after each amplification step were performed three times for 5 minutes with 2 ml of 1x wash buffer (ADC ref. 310091) at room temperature.

When FISH staining was combined to Immunofluorescence, the samples were washed twice for 5 minutes with 2ml of ddH_2O after SIGMAFAST™ incubation and then blocked with BSA 2%/PBS for 15 minutes at room temperature. eIF3B protein was then detected by using anti-eIF3B/EIF3S9 (#A301-761A, Bethyl, Montgomery, TX, USA) antibody diluted 1:100 in 1% BSA/1% goat serum/PBS overnight at 4 °C. Finally, the immunocomplexes were detected with Alexafluor 488-goat anti-rabbit secondary antibody (ThermoFisher A-11001) diluted 1:200 in 1% BSA/1% goat serum/PBS for 45 minutes at room temperature. After extensive washings with PBS, the cells were incubated with DAPI solution (Sigma, D9542; 1ug/ml/PBS) for 5 minutes at room temperature and then mounted using ProLong Diamond Antifade Mountant (ThermoFischer Scientific, P-36961). Samples were imaged on confocal microscopes (Spinning disk Olympus IX73 and laser scanning *FluoViewFV10i Olympus*) equipped with 60X NA1.35 oil (UPLANSApo) and water (UPLSAP) objectives respectively.

The Z-stacks (200 and 300 nm Z-spacing) were collected with MetaMorph or Fluoview software and merged with maximum intensity projection (MIP) method. All images were processed only in intensity threshold, contrast and brightness. Post-acquisition processing was applied using MetaMorph (Molecular Devices) and FIJI software to the entire image.

Supplementary references

53. Bolger AM, Lohse M, Usadel B. Trimmomatic: A flexible trimmer for Illumina sequence data. Bioinformatics. 2014;30(15):2114–20.
54. Zerbino DR, Achuthan P, Akanni W, Amode MR, Barrell D, Bhai J, et al. Ensembl 2018. Nucleic Acids Res. 2018;46(D1):D754–61.
55. Dobin A, Davis CA, Schlesinger F, Drenkow J, Zaleski C, Jha S, et al. STAR: Ultrafast universal RNA-seq aligner. Bioinformatics. 2013;29(1):15–21.
56. Anders S, Pyl PT, Huber W. HTSeq-A Python framework to work with high-throughput sequencing data. Bioinformatics. 2015;31(2):166–9.
57. Robinson MD, McCarthy DJ, Smyth GK. edgeR: A Bioconductor package for differential expression analysis of digital gene expression data. Bioinformatics. 2009;26(1):139–40.
58. Schurch NJ, Schofield P, Gierliński M, Cole C, Sherstnev A, Singh V, et al. How many biological replicates are needed in an RNA-seq experiment and which differential expression tool should you use? RNA. 2016 Jun;22(6):839–51.
59. Carbon S, Dietze H, Lewis SE, Mungall CJ, Munoz-Torres MC, Basu S, et al. Expansion of the gene ontology knowledgebase and resources: The gene ontology consortium. Nucleic Acids Res. 2017;45(D1):D331–8.
60. Zhang B, Kirov S, Snoddy J. WebGestalt: An integrated system for exploring gene sets in various biological contexts. Nucleic Acids Res. 2005;33(SUPPL. 2):741–8.
61. Geistlinger L, Csaba G, Zimmer R. Bioconductor's EnrichmentBrowser: Seamless navigation through combined results of set- & network-based enrichment analysis. BMC Bioinformatics. 2016;17(1):1–11.
62. Lachmann A, Giorgi FM, Lopez G, Califano A. ARACNe-AP: Gene network reverse engineering through adaptive partitioning inference of mutual information. Bioinformatics. 2016;32(14):2233–5.
63. Weinstein JN, Collisson EA, Mills GB, Shaw KM, Brad A, Ellrott K, et al. The cancer genome atlas pan-cancer analysis project. Nat Genet. 2013;45(10):1113–20